Number of virtual photons in the Coulomb dipole excitation

Kyoungsu Heo and Myung-Ki Cheoun
Department of Physics and Origin of Matter and Evolution of Galaxies (OMEG) Institute, Soongsil University, Seoul 06978, Korea

Ki-Seok Choi and K. S. Kim
School of Liberal Arts and Science, Korea Aerospace University, Koyang 10540, Korea

W. Y. So*
Department of Radiological Science, Kangwon National University at Dogye, Samcheok 25945, South Korea

(Received 9 April 2023; accepted 7 June 2023; published 20 June 2023)

In this study, the number of virtual photons obtained through general, relativistic, nonrelativistic, and intermediate methods was investigated, which is an important factor in obtaining the Coulomb dipole strength distribution. The number of virtual photons was studied according to the incident energy $E_{\rm lab}$ using five methods. The general method, which has two different forms (integral and differential), is valid for all energy regions, whereas the relativistic method is effective for regions with high β values. In addition, the validity of the nonrelativistic approximation was tested by comparing it with the general method in the low-incident-energy region, and the intermediate method was shown to be not effective in the high-excitation-energy region. Further, an investigation was conducted on the dependence of the number of virtual photons on the charges of the projectile and target nuclei. Using the same R value, target nuclei, and incident energy, it was found that the number of virtual photons does not depend on the charge number of the projectile in the relativistic method. With the same R value, projectile, and incident energy, in contrast it can be seen that the number of virtual photon depends on the square of the charge number of target nuclei.

DOI: 10.1103/PhysRevC.107.064608

I. INTRODUCTION

Nuclear physicists has long been interested in nuclear reactions involving the collision of a projectile and a target nucleus. In these nuclear reactions, two important interactions that determine the trajectory of the projectile are the nuclear and Coulomb forces. At a long distance, where the nuclear force does not reach, in general, the interaction between two nuclei is governed by the Coulomb force; therefore, the projectile follows the Coulomb trajectory [1,2]. However, as the distance between the projectile and target nucleus decreases, the projectile no longer follows the Coulomb trajectory owing to the influence of the attractive nuclear force.

In general, the charged projectile and target nucleus are excited by the Coulomb interaction generated between the two nuclei. This Coulomb excitation leads to pygmy dipole resonance (PDR) through the dipole vibration of valence neutron(s) on the core nucleus, whereas giant dipole resonance (GDR) is induced by the different phase motions of the neutrons relative to the protons in the nucleus [3,4]. In contrast to the GDR that occurs at high excitation energies, the PDR appears primarily at relatively low excitation energies. Since the 1980s, several experiments have been conducted using weakly bound nuclei as incident beams. Beams such as ^{6,8}He [5,6], ^{11}Li [7–9], and ^{11}Be [10–12] consist of neutron-rich nuclei containing more than one valence neutron. In addition, these incident beams have the feature that the valence neutron(s) can be easily separated by the Coulomb interaction from the core nuclei when the Coulomb excitation energy is greater than the neutron separation energy. This phenomenon, which emanates from Coulomb excitation, is called Coulomb dipole excitation (CDE) [13].

The importance of this CDE effect can be observed in the breakup reaction between a weakly bound projectile with valence neutron(s) and a heavy target nucleus [7–12]. For example, the ratio of the elastic scattering cross section ($\sigma_{\rm el}$) to that by the Rutherford scattering ($\sigma_{\rm RU}$), $P_E \equiv \sigma_{\rm el}/\sigma_{\rm RU}$, decreases rapidly at a forward angle (about $\theta_{\rm c.m.} \gtrsim 15^\circ$) for the ^{11}Li + ^{208}Pb system compared to ^{9}Li + ^{208}Pb one [7]. This shows that the projectile is already affected by the Coulomb and/or nuclear interaction in the long-range region (or large impact parameter region), such that the elastic scattering channel is switched to another channel related to the dissociation effect by $^{11}\text{Li} \rightarrow {}^{9}\text{Li} + 2n$. Considering that nuclear interactions only act in a short range, it is conjectured that this long-range effect is mainly caused by Coulomb interactions. Consequently, in the nuclear reaction between the weakly bound projectile with valence neutron(s) and the heavy target nucleus, measurement of the Coulomb dissociation cross section becomes very important.

*wyso@kangwon.ac.kr

Because the projectile and target do not interpenetrate, the electromagnetic interaction can be parametrized in terms of the electromagnetic matrix elements at the photon point, where the four-photon momentum $q^2 = \omega^2 - |\vec{q}\,|^2 = 0$. In contrast, the interaction between electrons and hadrons is determined by the exchange of a (spacelike) virtual photon, that is, $|\vec{q}\,| > \omega$. Moreover, for forward angle detection in low-energy nuclear reactions between the projectile and target, the four-photon momentum may approach zero; that is, the virtual photon can be treated as a real photon, particularly for large impact parameters.

In general, the excitation energy spectrum of the Coulomb dissociation cross section, $d\sigma_{\rm CD}/dE_{\rm x}$, for the $E1$ transition associated with the CDE is written as [14–16]

$$\frac{d\sigma_{\rm CD}}{dE_{\rm x}} = \frac{N_{E1}(E_{\rm x})}{E_{\rm x}}\sigma_{E1}(E_{\rm x}) = \frac{16\pi^3}{9\hbar c}N_{E1}(E_{\rm x})\frac{dB(E1)}{dE_{\rm x}}. \quad (1)$$

Here, $N_{E1}(E_{\rm x})$, expressed as a function of the excitation energy $E_{\rm x}$, is the number of virtual photon, and $\sigma_{E1}(E_{\rm x})$ is the total photonuclear cross section including the Coulomb dipole strength distribution, $dB(E1)/dE_{\rm x}$ [15,16]. More importantly, the dipole strength distribution is a significant factor in determining the strength of the CDE potential. Dipole strength distributions have been measured for several projectiles, such as ^{6}He [17], ^{11}Li [18], ^{11}Be [19–21], ^{19}B [22], and ^{15}C [23]. In Eq. (1), while the excitation energy spectrum of the Coulomb dissociation cross section can be measured directly, the experimental dipole strength distribution cannot be extracted directly. Instead, the dipole-strength distribution can be obtained using Eq. (1) after theoretically calculating the number of virtual photons for the $E1$ transition, $N_{E1}(E_{\rm x})$ [15,24,25].

In the present work, we closely examine the calculation of the number of virtual photons to extract the dipole strength distribution, which plays a crucially important role in the study of nuclear reactions for a weakly bound projectile with valence neutron(s). To this end, we theoretically calculated the number of virtual photons obtained under several conditions (general, relativistic, intermediate, and nonrelativistic) and compared them with each other.

II. NUMBER OF VIRTUAL PHOTONS

Generally, both the projectile and target nuclei are excited by the Coulomb and nuclear interactions between the two nuclei. In the present work, however, we only considered the excitation of the projectile because we focused on calculating the number of virtual photons related to the Coulomb dissociation of the weakly bound projectile with the valence neutron(s).

The number of virtual photons $N_{E1}(E_{\rm x})$ is calculated by solving the Schrödinger equation including a first-order perturbation theory. The final form is obtained by integrating the equation

$$\begin{aligned}\frac{dN_{E1}(E_{\rm x},\Omega)}{d\Omega} &= \frac{Z_t^2\alpha}{4\pi^2}\left(\frac{c}{v}\right)^2\varepsilon^4\zeta^2 e^{-\pi\zeta}\left\{\frac{\varepsilon^2-1}{\varepsilon^2}[K_{i\zeta}(\varepsilon\zeta)]^2 + [K'_{i\zeta}(\varepsilon\zeta)]^2\right\}\\ &= \frac{Z_t^2\alpha}{4\pi^2}\left(\frac{c}{v}\right)^2\varepsilon^4\eta^2 e^{-\pi\eta}\left\{\frac{1}{\gamma^2}\frac{\varepsilon^2-1}{\varepsilon^2}[K_{i\eta}(\varepsilon\eta)]^2 + [K'_{i\eta}(\varepsilon\eta)]^2\right\} \quad (2)\end{aligned}$$

with respect to solid angle Ω [15,16]. Here, Z_t and α are the target charge number and the fine structure constant, respectively. Also, $\varepsilon = 1/\sin(\theta/2)$ is the eccentricity parameter of the Coulomb orbit related to the scattering angle θ [16] and $\zeta = \gamma\eta$ is an adiabaticity parameter consisting of the product of $\gamma = 1/\sqrt{1 - v^2/c^2}$ and the Sommerfeld parameter, $\eta = a_0 E_{\rm x}/\hbar v$. Note that a_0 and $E_{\rm x}$ are the distance of closest approach in a head-on collision and the excitation energy given by the virtual photon energy, respectively [16,26,27]. v is the projectile velocity related to the incident energy. $K_{i\zeta}(\varepsilon\zeta)$ and $K'_{i\zeta}(\varepsilon\zeta)$ are modified Bessel functions of imaginary order and derivative type, respectively. As detailed in Ref. [15], integrating Eq. (2) for all the eccentric parameters ε can be written as follows [15,16]:

$$N_{E1}(E_{\rm x}) = \frac{2Z_t^2\alpha}{\pi}\eta^2 e^{-\pi\eta}\left(\frac{c}{v}\right)^2\int_{\varepsilon_0}^{\infty}\varepsilon\, d\varepsilon\left\{\frac{1}{\gamma^2}\frac{\varepsilon^2-1}{\varepsilon^2}[K_{i\eta}(\varepsilon\eta)]^2 + [K'_{i\eta}(\varepsilon\eta)]^2\right\}, \quad (3)$$

where $\varepsilon_0 = 1$ for $E \leqslant E_B$ and $\varepsilon_0 = \sqrt{1 + 4(E/E_B)^2(1 - E_B/E)}$ for $E > E_B$. Here E and E_B are the incident (or bombardment) and Coulomb barrier energies, respectively.

First, if the incident energy of the projectile is significantly higher than the Coulomb barrier energy, $E \gg E_B$, then $\varepsilon_0 \approx 2E/E_B = R/a_0$. R is the sum of the projectile and target radii. Consequently, integrating Eq. (3) can be expressed as [15,16]

$$\begin{aligned}N_{E1}(E_{\rm x}) = \frac{2Z_t^2\alpha}{\pi}\eta^2 e^{-\pi\eta}\left(\frac{c}{v}\right)^2\Bigg\{&-\xi K_{i\eta}(\xi)K_{i\eta}(\xi) - \frac{1}{2}\left(\frac{c}{v}\right)^{-2}\xi^2\Bigg[K_{i\eta+1}(\xi)K_{i\eta-1}(\xi)\\ &- K_{i\eta}^2(\xi) + \frac{1}{\varepsilon_0}\left(K_{i\eta}(\xi)\left\langle\frac{\partial K'_{i\eta}(\xi)}{\partial\mu}\right\rangle_{\mu=i\eta} - K'_{i\eta}(\xi)\left\langle\frac{\partial K_{i\eta}(\xi)}{\partial\mu}\right\rangle_{\mu=i\eta}\right)\Bigg]\Bigg\}. \quad (4)\end{aligned}$$

Here $\xi = \varepsilon_0\eta$. For reference, refer to Eqs. (3) and Eq. (4) as general methods with integral and differential forms, respectively.

From the relativistic limit $\beta \to 1$ ($\varepsilon_0 \approx R/a_0 \to \infty$, $\eta = \zeta/\gamma \to 0$) and nonrelativistic limit $\beta \to 0$ ($\varepsilon_0 \to 1$), Eq. (3) can be rewritten as follows [15,16]:

$$N_{E1}(E_x) = \frac{2Z_t^2\alpha}{\pi}\left(\frac{c}{v}\right)^2\left\{\xi K_0(\xi)K_1(\xi) - \frac{v^2\xi^2}{2c^2}\left[K_1^2(\xi) - K_0^2(\xi)\right]\right\} \tag{5}$$

and

$$N_{E1}(E_x) = -\frac{2Z_t^2\alpha}{\pi}\zeta e^{-\pi\zeta}\left(\frac{c}{v}\right)^2 K_{i\zeta}(\zeta)K'_{i\zeta}(\zeta). \tag{6}$$

Similarly, we refer to Eqs. (5) and (6) as the relativistic and nonrelativistic methods, respectively.

For an intermediate energy of tens of MeV per nucleon, the number of virtual photons can be expressed as follows [24]:

$$\begin{aligned} N_{E1}(E_x) = \frac{2Z_t^2\alpha}{\pi}e^{-\pi\eta}\left(\frac{c}{v}\right)^2\Bigg\{&\left(1 - 2\eta^2 + \frac{\eta^2}{\xi}\right)\ln\left(\frac{\delta}{\xi}\right) - \xi\eta^2\left[\frac{1}{\xi^2} + \ln^2\left(\frac{\delta}{\xi}\right)\right] \\ &- \frac{1}{2}\left(\frac{c}{v}\right)^{-2}\xi^2\left[\frac{1}{\xi^2} - \ln^2\left(\frac{\delta}{\xi}\right) + \eta^2\left(\frac{1}{\xi^2}\ln^2\left\langle\frac{\delta}{\xi}\right\rangle + 2\ln^2\left\langle\frac{\delta}{\xi}\right\rangle + 2\frac{\xi-1}{\xi}\right)\right]\Bigg\}. \end{aligned} \tag{7}$$

Here, we used $\delta = 1.123$, as noted in Ref. [24]. Also, Eq. (7) corresponds to the intermediate method.

III. RESULTS

A. Incident energy dependency of the projectile

First, to ensure the reliability of our calculations, we compared our results with previous studies by other research groups [25,28,29]. Figure 1(a) shows the number of virtual photons obtained from the general, relativistic, and intermediate methods at $E_{lab} = 28$ MeV/nucleon for ^{11}Li projectile compared to those calculated from Ref. [25]. The solid black and dashed red lines were extracted using the general method in the integral and differential forms [Eqs. (3) and (4)]. The dotted blue, dash-dotted green, and dash-dot-dotted magenta lines were extracted using the general method in the relativistic [Eq. (5)], nonrelativistic [Eq. (6)], and intermediate [Eq. (7)] methods, respectively. As shown in the figure, it can be seen that the number of virtual photons we calculated is in good agreement with the general (black squares), relativistic (green circles), and intermediate (violet stars) methods calculated in Ref. [25]. Therefore, we believe that the results of our calculations are reliable.

Based on these results, we calculated the number of virtual photons obtained using the five methods described in Fig. 1(b). As shown in the figure, the numbers of virtual photons obtained by both general methods (integral and differential forms) are highly consistent with each other. This means that it does not matter whether one uses either the integral or differential form in the general method. In our calculations after this, we use the general method given by Eq. (4) in the differential form.

The dotted blue line indicates the number of virtual photons obtained using the relativistic method. Note that, as the virtual photon energy (E_x) increases, the difference in the number of virtual photons generated by the general and relativistic methods gradually increases at $E_{lab} =$ 28 MeV/nucleon. As mentioned previously, the relativistic method is calculated under the condition that the β value is close to unity. Because the β value corresponding to $E_{lab} =$ 28 MeV/nucleon was approximately 0.24, it did not reach the relativistic limit. Consequently, the difference between general and relativistic methods arises from this approximation. To take a closer look at the differences in the number of virtual photons obtained by the two methods, we considered the incident energy of the projectile with $E_{lab} = 280$ MeV/nucleon ($\beta \approx 0.64$), which is ten times larger. As shown in Fig. 1(c), the differences in the number of virtual photons obtained from the two methods are indistinguishable. This means that, if it is close to the relativistic limit, there is no problem using the relativistic approximation instead of the general method at $E_{lab} = 280$ MeV/nucleon. To examine the consistency between the general and relativistic methods at high incident energies, we chose an incident energy whose β value was close to unity, and compared the number of virtual photons obtained using the two methods. As shown in Fig. 1(d), plotted for the number of virtual photons obtained using the two methods, this consistency can be observed more clearly at $E_{lab} = 2800$ MeV/nucleon ($\beta \approx 0.97$). In fact, as mentioned in Ref. [25], the difference between general and relativistic methods is approximately 2%.

The dash-dotted green line represents the number of virtual photons obtained using the nonrelativistic method [Eq. (6)]. As shown in Figs. 1(c) and 1(d), it can be seen that the number of virtual photons obtained from the nonrelativistic method is relatively greater than that obtained from the general method. This is also inferred to be different from the nonrelativistic approximation ($\beta \to 0$). In fact, it cannot be stated that β values corresponding to the incident projectile energies at $E_{lab} = 28$ and 280 MeV/nucleon were close to 0. To examine the consistency between the general and nonrelativistic methods at low incident energies, we selected an incident energy whose β value was close to zero and compared the number of virtual photons obtained using the two methods. Therefore, we selected an incident projectile energy ($E_{lab} = 2.8$ MeV/nucleon) with $\beta \approx 0.01$, which is close to zero, as plotted in Fig. 1(e). Consequently, the numbers of virtual photons obtained using the two methods were, expectedly, almost identical.

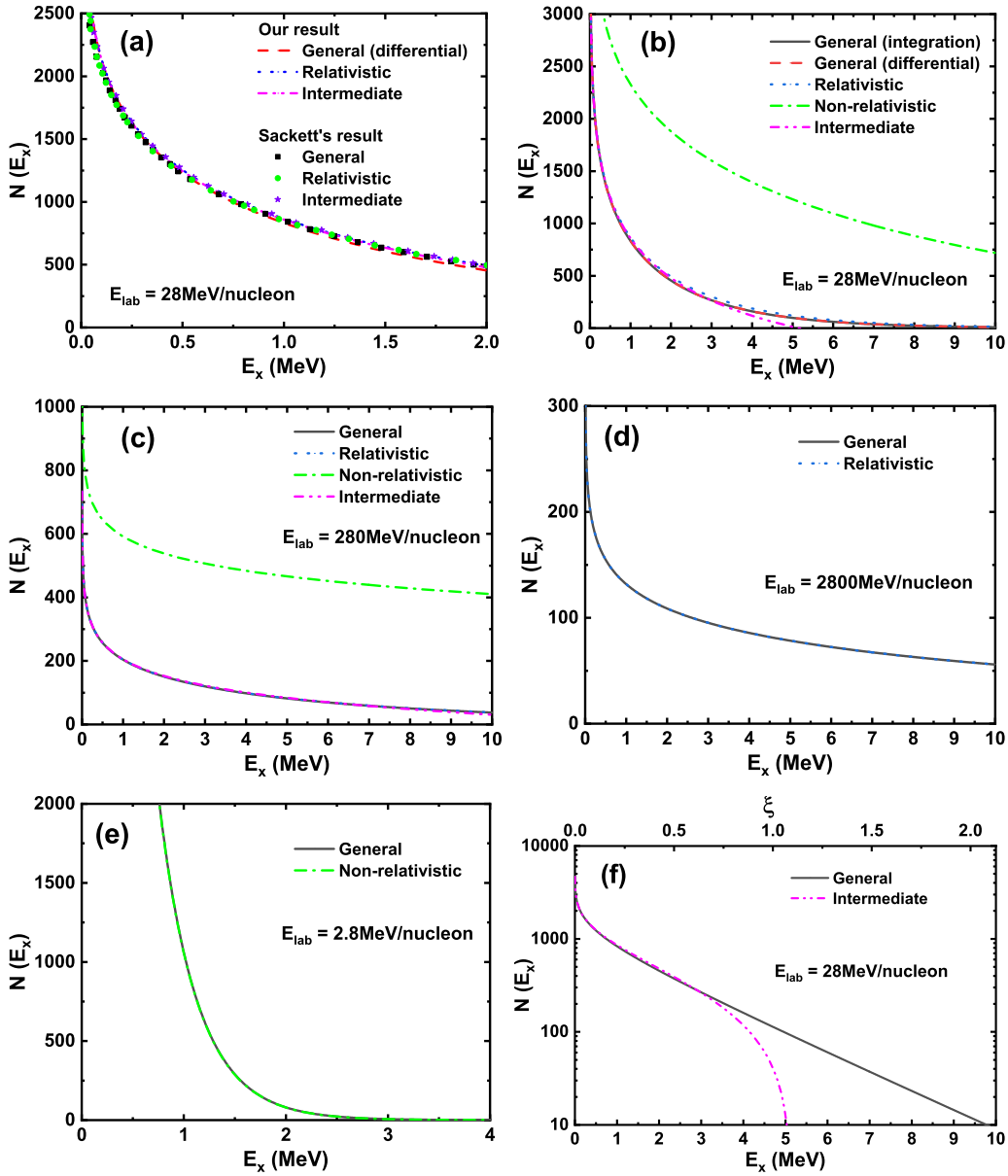

FIG. 1. The number of virtual photons for the $^{11}\mathrm{Li} + {}^{208}\mathrm{Pb}$ system at $E_{\mathrm{lab}} = 2.8$, 28, 280, and 2800 MeV/nucleon. The solid black and dashed red lines represent the results obtained from the general method with integral and differential form, respectively, while the dotted blue, dash-dotted green, and dash-dot-dotted magenta lines correspond to the relativistic, nonrelativistic, and intermediate methods, respectively. See the text for details. Additionally, the black squares, green circles, and violet stars represent results obtained using the general, relativistic, and intermediate methods by Sackett [25]. Note that we use the $R = 10.3$ fm [25].

Finally, the dashed-dotted magenta line represents the number of virtual photons obtained using the intermediate method [Eq. (7)]. As shown in Fig. 1(b), it can be seen that the numbers of photons obtained from the general and intermediate methods differ approximately at $E_{\mathrm{x}} > 0.75$ MeV, but it is not clearly visible on a linear scale. Therefore, if redrawn on a logarithmic scale, as shown in Fig. 1(f), the differences between the two methods can be clearly observed. In Ref. [24], the following approximation was applied to the intermediate method: $\xi = \varepsilon_0 \eta \ll 1$. In fact, at $E_{\mathrm{x}} \leqslant 0.75$ MeV corresponding to $\xi \leqslant 0.16$, the number of virtual photon obtained by the two methods is similar, but its difference increases as the excitation energy (or the adiabaticity parameter) increases. Therefore, it can be inferred that the intermediate method is not effective in the high excitation energy region.

For reference, based on the calculation results so far, the percentage differences between the relativistic method and the general one given by $\frac{|N(E_{\mathrm{x}})_{\mathrm{rel}} - N(E_{\mathrm{x}})_{\mathrm{gen}}|}{[N(E_{\mathrm{x}})_{\mathrm{rel}} + N(E_{\mathrm{x}})_{\mathrm{gen}}]/2} \times 100(\%)$ for $E_{\mathrm{lab}} = 28$, 280, and 2800 MeV/nucleon are about 4% (20%, 39%), 0.1% (0.6%, 1.2%), and 0.002% (0.01%, 0.02%), respectively, at $E_{\mathrm{x}} = 1$ MeV (5 MeV, 10 MeV). It means that the relativistic method does not work in low incident energy region. On the other hand, the percentage difference between the nonrelativistic method and the general one for $E_{\mathrm{lab}} = 2.8$, 28,

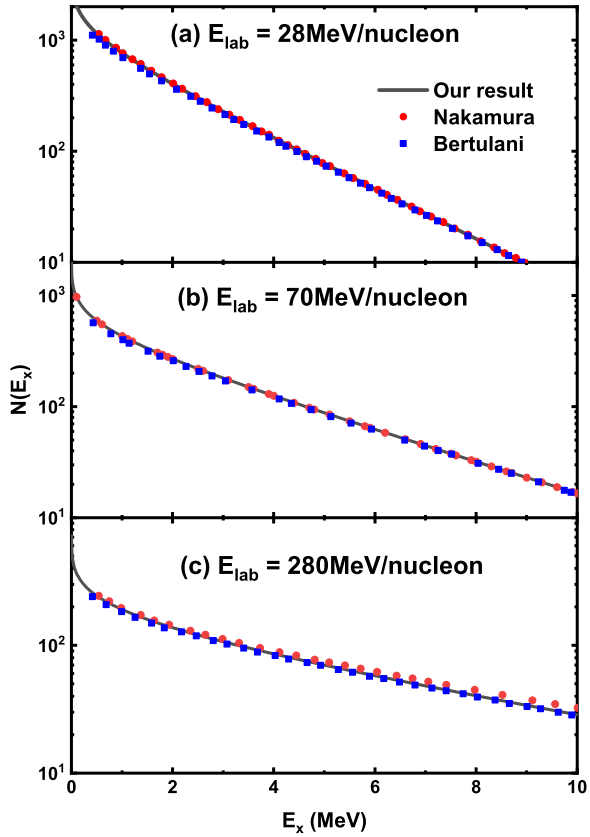

FIG. 2. The same as Fig. 1 but for $R = 12.3$ fm at (a) $E_{\rm lab} =$ 28 MeV/nucleon, (b) $E_{\rm lab} = 70$ MeV/nucleon, and (c) $E_{\rm lab} =$ 280 MeV/nucleon of the $^{11}{\rm Li} + {}^{208}{\rm Pb}$ system. The solid black lines are our present result. Additionally, the red circles and blue squares are the results obtained by Nakamura [29] and Bertulani [28], respectively, as reported in Refs. [28–30]. Note that the relativistic method is used to obtain the number of virtual photons in these calculations. Nakamura data were obtained through private communication [30].

and 280 MeV/nucleon are about 1% (3%, 6%), 95% (171%, 195%), and 97% (140%, 167%), respectively, at $E_{\rm x} = 1$ MeV (5 MeV, 10 MeV). Therefore, nonrelativistic approach is not good for the energy region of tens and hundreds of MeV. Regarding the intermediate method, since the number of virtual photons changes rapidly with respect to the excitation energy ($E_{\rm x}$) as shown in Fig. 1(f), it seems meaningless to find the percentage difference between the intermediate method and the general one, so it is omitted.

We can examine the reliability of our calculations by referring to other studies [28,29]. Figure 2 shows the number of virtual photons obtained using the relativistic method at $E_{\rm lab} = 28$, 70, and 280 MeV/nucleon, respectively. For reference, if the target nucleus is the same, the number of virtual photons obtained from the relativistic method is always the same regardless of the type of projectile [28]. As shown in Fig. 2, it can be seen that our results are almost identical to those of Bertulani and Nakamura. However, for the number of virtual photons used at $E_{\rm lab} = 70$ MeV/nucleon, we used the data directly received from the Nakamura group [30] instead of those obtained from Fig. 2.3 of Ref. [29].

B. Charge dependency of the projectile and target nucleus

In this section, we examine the dependence of the projectile and target nuclei on the number of virtual photons. As mentioned earlier, the number of virtual photons obtained is the same for a given target nucleus, regardless of the projectile type used. If we assume that the incident energy per nucleon is the same, then the velocity of the projectiles will be the same. In Eq. (5), therefore, at the same R value, the parameter $\xi = \frac{E_{\rm x}R}{\gamma\hbar v}$ expressed as a function of velocity will be the same. Consequently, the same value was obtained for the number of virtual photons [28].

Figure 3(a) shows the number of virtual photons for various projectiles with respect to $R = 12.3$ fm and ^{208}Pb target at $E_{\rm lab} = 70$ MeV/nucleon. The solid black, dashed red, dotted blue, and dash-dotted green lines represent the number of virtual photons for ^{11}Li, ^{11}Be, ^{16}O, and ^{40}Ca nuclei, respectively. As mentioned previously, there is no dependence on the type of projectile used. Figure 3(b) shows the number of virtual photons for various target nuclei with respect to $R = 12.3$ fm and ^{11}Li projectile at $E_{\rm lab} = 70$ MeV/nucleon. The solid black, dashed red, dotted blue, dash-dotted green, and dash-dotted lines represent the number of virtual photons for ^{28}Si, ^{58}Ni, ^{144}Sm, ^{197}Au, and ^{208}Pb nuclei, respectively. In Eq. (5), the number of virtual photons depends on the square of the target nuclei's charge number. Therefore, we extract the number of virtual photons at $E_{\rm x} = 2$MeV and find $N_{E1}(E_{\rm x}) = 7.845$, 31.382, 153.866, 249.812, and 269.146 for ^{28}Si, ^{58}Ni, ^{144}Sm, ^{197}Au, and ^{208}Pb nuclei, respectively. If we set the number of virtual photons to $N_{E1}(E_{\rm x}) = 0.04\ Z_t^2$ and substitute the charge number of each projectile, we obtain $N_{E1}(E_{\rm x}) = 7.84$, 31.36, 153.76, 249.64, and 268.96 for ^{28}Si, ^{58}Ni, ^{144}Sm, ^{197}Au, and ^{208}Pb nuclei, respectively. The number of virtual photons obtained from a simple approximation is similar to that obtained using the relativistic method. This only applies to a specific excitation energy ($E_{\rm x} = 2$MeV); however, if the excitation energy changes, then a factor of 0.04 is no longer available. For reference, we arbitrarily selected light to heavy nuclei as target nuclei, which were ^{28}Si, ^{58}Ni, ^{144}Sm, ^{197}Au, and ^{208}Pb nuclei.

C. Application for the Coulomb dipole strength distribution, $dB(E1)/dE_{\rm x}$

Thus far, we have calculated the number of photons using various methods. As mentioned above, the number of virtual photons is calculated to determine the Coulomb dipole strength distribution, $dB(E1)/dE_{\rm x}$, from the excitation energy spectrum of the Coulomb dissociation cross section, $d\sigma_{\rm CD}/dE_{\rm x}$. So, we will try to calculate the Coulomb dipole strength distribution by applying various methods to obtain the number of virtual photons in a specific system ($^{19}{\rm B} + {}^{208}{\rm Pb}$ system).

Figure 4(a) shows the number of virtual photons at $E_{\rm lab} =$ 220 MeV/nucleon for the $^{19}{\rm B} + {}^{208}{\rm Pb}$ system using the general (solid black), relativistic (dashed blue), and nonrelativistic (dash-dotted green) methods. Owing to the high incident energy, the numbers of virtual photons obtained from the two methods were almost the same, except for that

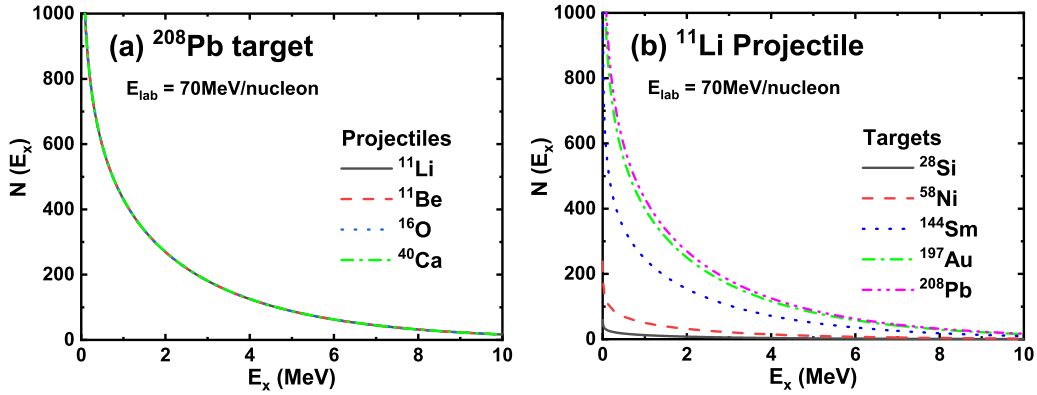

FIG. 3. The same as Fig. 1 but for (a) various projectiles with $R = 12.3$ fm and ^{208}Pb target and (b) various target nuclei with $R = 12.3$ fm and ^{11}Li projectile at $E_{\rm lab} = 70$ MeV/nucleon. Note that the relativistic method is used to obtain the number of virtual photons in these calculations.

obtained from the nonrelativistic method. Figure 4(b) shows the Coulomb dipole strength distribution extracted from these virtual photons using $R = 11.17$ fm. For this calculation, we did not use the experimental two-neutron separation energy $S_{2n}^{\rm exp} = 0.089$ MeV, but applied $S_{2n} = 0.5$ MeV, as in Ref. [22]. Consequently, we obtained three types of Coulomb dipole strength distributions. With the exception of the nonrelativistic method (green stars), all of the other methods produce Coulomb dipole strength distributions that closely match the experimental distribution obtained from Ref. [22]. In particular, the experimental Coulomb dipole strength distribution obtained using the relativistic method (red circles) and our results obtained using the same method (blue triangles) are almost identical, as shown in Fig. 4(b). Therefore, our results for the number of virtual photons are reliable.

IV. SUMMARY AND CONCLUSION

We studied the number of virtual photons obtained from general, relativistic, nonrelativistic, and intermediate methods. The number of virtual photons is a very important factor in obtaining the Coulomb dipole strength distribution, $dB(E1)/dE_{\rm x}$, from the excitation energy spectrum of the Coulomb dissociation cross section.

First, we compared the results for the number of virtual photons obtained from other research groups, and the reliability of our results was confirmed because they were reproduced well.

Next, we investigated the number of virtual photons according to the incident energy $E_{\rm lab}$. The general method is valid for all energy regions, whereas the relativistic method is effective for regions with high β values. However, because the difference between the two methods is not large (approximately 2%), it is confirmed that there will be no problem even if the relativistic method is used instead of the general method for convenience. In addition, the validity of the nonrelativistic approximation was confirmed by comparing it with the general method in the low-incident-energy region. Because the intermediate method is applied to the approximation $\xi = \varepsilon_0\eta \ll 1$, we can infer that the intermediate method is ineffective in the high-excitation-energy region.

Finally, we investigated the dependence of the number of virtual photons on the charge numbers of the projectile

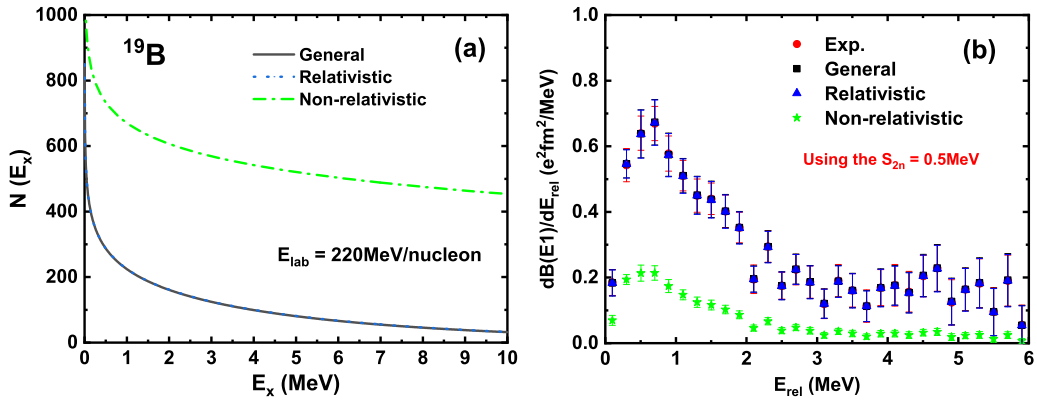

FIG. 4. (a) The number of virtual photons and (b) the Coulomb dipole strength distribution at $E_{\rm lab} = 220$ MeV/nucleon for the ^{19}B + ^{208}Pb system using various methods. Note that we use $R = 11.17$ fm and two-neutron separation energy $S_{2n} = 0.5$ MeV instead of the experimental value $S_{2n}^{\rm exp} = 0.089$ MeV [22].

and target nuclei. Using the same R value, target nuclei, and incident energy, we observed that the number of virtual photons in the relativistic method was independent of the charge number of the projectile. However, with the same R value, projectile, and incident energy, we found that the number of virtual photons depends on the square of charge number of target nuclei.

ACKNOWLEDGMENTS

This study was supported by the National Research Foundation of Korea (Grants No. NRF-2020R1A2C3006177, No. NRF-2021R1A6A1A03043957, No. NRF-2021R1F1A1046575, and No. NRF-2021R1F1A1051935) and by MSIT (Grant No. 2018R1A5A1025563).

[1] R. Bass, *Nuclear Reactions with Heavy Ions* (Springer-Verlag, New York, 1980).

[2] B. T. Kim, W. Y. So, S. W. Hong, and T. Udagawa, Phys. Rev. C **65**, 044607 (2002).

[3] D. Gambacurta, in *Proceedings of the Carpathian Summer School of Physics 2018 (CSSP18), 1–14 July 2018, Sinaia, Romania*, edited by L. Trache and A. Spiridon, AIP Conf. Proc. No. 2076 (AIP, New York, 2019), p. 040003.

[4] N. Q. Hung, H. A. T. Kiet, H. N. Duc, and N. T. Chuong, J. Phys.: Conf. Ser. **726**, 012026 (2016).

[5] E. F. Aguilera, J. J. Kolata, F. D. Becchetti, P. A. DeYoung, J. D. Hinnefeld, Á. Horváth, L. O. Lamm, H.-Y. Lee, D. Lizcano, E. Martinez-Quiroz, P. Mohr, T. W. O'Donnell, D. A. Roberts, and G. Rogachev, Phys. Rev. C **63**, 061603(R) (2001).

[6] A. Lemasson, A. Navin, N. Keeley, M. Rejmund, S. Bhattacharyya, A. Shrivastava, D. Bazin, D. Beaumel, Y. Blumenfeld, A. Chatterjee, D. Gupta, G. de France, B. Jacquot, M. Labiche, R. Lemmon, V. Nanal, J. Nyberg, R. G. Pillay, R. Raabe, K. Ramachandran *et al.*, Phys. Rev. C **82**, 044617 (2010).

[7] M. Cubero, J. P. Fernández-García, M. Rodríguez-Gallardo, L. Acosta, M. Alcorta, M. A. G. Alvarez, M. J. G. Borge, L. Buchmann, C. A. Diget, H. A. Falou, B. R. Fulton, H. O. U. Fynbo, D. Galaviz, J. Gómez-Camacho, R. Kanungo, J. A. Lay, M. Madurga, I. Martel, A. M. Moro, I. Mukha *et al.*, Phys. Rev. Lett. **109**, 262701 (2012).

[8] J. P. Fernández-García, M. Cubero, M. Rodríguez-Gallardo, L. Acosta, M. Alcorta, M. A. G. Alvarez, M. J. G. Borge, L. Buchmann, C. A. Diget, H. A. Falou, B. R. Fulton, H. O. U. Fynbo, D. Galaviz, J. Gómez-Camacho, R. Kanungo, J. A. Lay, M. Madurga, I. Martel, A. M. Moro, I. Mukha *et al.*, Phys. Rev. Lett. **110**, 142701 (2013).

[9] A. M. Vinodkumar, W. Loveland, R. Yanez, M. Leonard, L. Yao, P. Bricault, M. Dombsky, P. Kunz, J. Lassen, A. C. Morton, D. Ottewell, D. Preddy, and M. Trinczek, Phys. Rev. C **87**, 044603 (2013).

[10] A. Di Pietro, G. Randisi, V. Scuderi, L. Acosta, F. Amorini, M. J.G. Borge, P. Figuera, M. Fisichella, L. M. Fraile, J. Gomez-Camacho, H. Jeppesen, M. Lattuada, I. Martel, M. Milin, A. Musumarra, M. Papa, M. G. Pellegriti, F. Perez-Bernal, R. Raabe, F. Rizzo, D. Santonocito, G. Scalia, O. Tengblad, D. Torresi, A. M. Vidal, D. Voulot, F. Wenander, and M. Zadro, Phys. Rev. Lett. **105**, 022701 (2010).

[11] A. Di Pietro, V. Scuderi, A. M. Moro, L. Acosta, F. Amorini, M. J.G. Borge, P. Figuera, M. Fisichella, L. M. Fraile, J. Gomez-Camacho, H. Jeppesen, M. Lattuada, I. Martel, M. Milin, A. Musumarra, M. Papa, M. G. Pellegriti, F. Perez-Bernal, R. Raabe, G. Randisi, F. Rizzo, G. Scalia, O. Tengblad, D. Torresi, A. M. Vidal, D. Voulot, F. Wenander, and M. Zadro, Phys. Rev. C **85**, 054607 (2012).

[12] L. Acosta *et al.*, Eur. Phys. J. A **42**, 461 (2009).

[13] J. P. Fernández-García, M. Cubero, L. Acosta, M. Alcorta, M. A.G. Alvarez, M. J.G. Borge, L. Buchmann, C. A. Diget, H. A. Falou, B. Fulton, H. O.U. Fynbo, D. Galaviz, J. Gomez-Camacho, R. Kanungo, J. A. Lay, M. Madurga, I. Martel, A. M. Moro, I. Mukha, T. Nilsson, M. Rodriguez-Gallardo, A. M. Sanchez-Benitez, A. Shotter, O. Tengblad, and P. Walden, Phys. Rev. C **92**, 044608 (2015).

[14] K. Alder and A. Winther, *Electromagnetic Excitation* (North-Holland, Amsterdam, 1975).

[15] C. A. Bertulani and G. Baur, Phys. Rep. **163**, 299 (1988).

[16] D. Sackett, K. Ieki, A. Galonsky, C. A. Bertulani, H. Esbensen, J. J. Kruse, W. G. Lynch, D. J. Morrissey, N. A. Orr, B. M. Sherrill, H. Schulz, A. Sustich, J. A. Winger, F. Deák, Á. Horváth, Á. Kiss, Z. Seres, J. J. Kolata, R. E. Warner, and D. L. Humphrey, Phys. Rev. C **48**, 118 (1993).

[17] T. Aumann, D. Aleksandrov, L. Axelsson, T. Baumann, M. J. G. Borge, L. V. Chulkov, J. Cub, W. Dostal, B. Eberlein, Th. W. Elze, H. Emling, H. Geissel, V. Z. Goldberg, M. Golovkov, and A. Grünschloß M. Hellström, K. Hencken, J. Holeczek, R. Holzmann, B. Jonson, A. A. Korshenninikov *et al.*, Phys. Rev. C **59**, 1252 (1999).

[18] T. Nakamura, A. M. Vinodkumar, T. Sugimoto, N. Aoi, H. Baba, D. Bazin, N. Fukuda, T. Gomi, H. Hasegawa, N. Imai, M. Ishihara, T. Kobayashi, Y. Kondo, T. Kubo, M. Miura, T. Motobayashi, H. Otsu, A. Saito, H. Sakurai, S. Shimoura *et al.*, Phys. Rev. Lett. **96**, 252502 (2006).

[19] T. Nakamura, S. Shimoura, T. Kobayashi, T. Teranishi, K. Abe, N. Aoi, Y. Doki, M. Fujimaki, N. Inabe, N. Iwasa, K. Katori, T. Kubo, H. Okuno, T. Suzuki, I. Tanihata, Y. Watanabe, A. Yoshida, and M. Ishihara, Phys. Lett. B **331**, 296 (1994).

[20] R. Palit, P. Adrich, T. Aumann, K. Boretzky, B. V. Carlson, D. Cortina, U. Datta Pramanik, Th. W. Elze, H. Emling, H. Geissel, M. Hellström, K. L. Jones, J. V. Kratz, R. Kulessa, Y. Leifels, A. Leistenschneider, G. Münzenberg, C. Nociforo, P. Reiter, H. Simon, K. Sümer, and W. Walus, Phys. Rev. C **68**, 034318 (2003).

[21] N. Fukuda, T. Nakamura, N. Aoi, N. Imai, M. Ishihara, T. Kobayashi, H. Iwasaki, T. Kubo, A. Mengoni, M. Notani, H. Otsu, H. Sakurai, S. Shimoura, T. Teranishi, Y. X. Watanabe, and K. Yoneda, Phys. Rev. C **70**, 054606 (2004).

[22] K. J. Cook, T. Nakamura, Y. Kondo, K. Hagino, K. Ogata, A. T. Saito, N. L. Achouri, T. Aumann, H. Baba, F. Delaunay, Q. Deshayes, P. Doornenbal, N. Fukuda, J. Gibelin, J. W. Hwang, N. Inabe, T. Isobe, D. Kameda, D. Kanno, S. Kim *et al.*, Phys. Rev. Lett. **124**, 212503 (2020).

[23] T. Nakamura, N. Fukuda, N. Aoi, N. Imai, M. Ishihara, H. Iwasaki, T. Kobayashi, T. Kubo, A. Mengoni, T. Motobayashi,

M. Notani, H. Otsu, H. Sakurai, S. Shimoura, T. Teranishi, Y. X. Watanabe, and K. Yoneda, Phys. Rev. C **79**, 035805 (2009).
[24] M. S. Hussein, M. P. Pato, and C. A. Bertulani, Phys. Rev. C **44**, 2219 (1991).
[25] D. Sackett, Ph.D. dissertation, Michigan State University, 1992 (unpublished).
[26] M. V. Andrés, J. Gómez-Camacho, and M. A. Nagarajan, Nucl. Phys. A **579**, 273 (1994).
[27] M. V. Andrés and J. Gómez-Camacho, Phys. Rev. Lett. **82**, 1387 (1999).
[28] C. A. Bertulani, arXiv:0908.4307.
[29] T. Nakamura and Y. Kondo, in *Clusters in Nuclei, Vol. 2*, Lecture Notes in Physics Vol. 848 (Springer-Verlag, Berlin, 2012), p. 67.
[30] We recently obtained new data on the number of virtual photons at $E_{\rm lab} = 70$MeV/nucleon through private communication with the Nakamura group.